8116 J. Med. Chem. 2010, 53, 8116–8128
DOI: 10.1021/jm101010n

Journal of Medicinal Chemistry Article

Synthesis and Discovery of Water-Soluble Microtubule Targeting Agents that Bind to the Colchicine Site on Tubulin and Circumvent Pgp Mediated Resistance

Aleem Gangjee,*[,†,∥] Ying Zhao,[†] Lu Lin,[†] Sudhir Raghavan,[†] Elizabeth G. Roberts,[‡] April L. Risinger,[‡] Ernest Hamel,[§] and Susan L. Mooberry*[,‡,∥]

[†]*Division of Medicinal Chemistry, Graduate School of Pharmaceutical Sciences, Duquesne University, 600 Forbes Avenue, Pittsburgh, Pennsylvania 15282, United States,* [‡]*Department of Pharmacology, University of Texas Health Science Center at San Antonio, 7703 Floyd Curl Drive, San Antonio, Texas 78229, United States, and* [§]*Screening Technologies Branch, Developmental Therapeutics Program, Division of Cancer Treatment and Diagnosis, National Cancer Institute at Frederick, National Institutes of Health, Frederick, Maryland 21702, United States.* [∥]*These authors contributed equally to this work*

Received August 4, 2010

Two classes of molecules were designed and synthesized based on a 6-CH_3 cyclopenta[*d*]pyrimidine scaffold and a pyrrolo[2,3-*d*]pyrimidine scaffold. The pyrrolo[2,3-*d*]pyrimidines were synthesized by reacting ethyl 2-cyano-4,4-diethoxybutanoate and acetamidine, which in turn was chlorinated and reacted with the appropriate anilines to afford **1** and **2**. The cyclopenta[*d*]pyrimidines were obtained from 3-methyladapic acid, followed by reaction with acetamidine to afford the cyclopenta[*d*]pyrimidine scaffold. Chlorination and reaction with appropriate anilines afforded (±)-**3**·HCl−(±)-**7**·HCl. Compounds **1** and (±)-**3**·HCl had potent antiproliferative activities in the nanomolar range. Compound (±)-**3**·HCl is significantly more potent than **1**. Mechanistic studies showed that **1** and (±)-**3**·HCl cause loss of cellular microtubules, inhibit the polymerization of purified tubulin, and inhibit colchicine binding. Modeling studies show interactions of these compounds within the colchicine site. The identification of these new inhibitors that can also overcome clinically relevant mechanisms of drug resistance provides new scaffolds for colchicine site agents.

Introduction

Three major classes of microtubule active agents have been identified (Figure 1).[1−3] The vinca alkaloids vincristine, vinblastine, vindesine, and vinorelbine are β-tubulin binding agents that are important in the treatment of leukemias, lymphomas, non-small-cell lung cancer, and other cancers. These are microtubule polymerization inhibitors. The second group includes the taxoids, paclitaxel (Taxol) and docetaxel (Taxotere), as well as the epothilones. The binding site for paclitaxel is also in the β-subunit but is distinct from that of the vinca alkaloids. Paclitaxel and other taxoids (and the epothilones) bind to the interior of the microtubule,[4,5] and these are designated microtubule-stabilizing agents becuase they stimulate tubulin polymerization. The taxoids are useful in the treatment of breast, lung, ovarian, head and neck, and prostate carcinomas among others. The third class, typified by colchicine, is composed of a diverse collection of small molecules that bind to the colchicine site on β-tubulin at its interface with α-tubulin, distinct from the vinca site. Colchicine site agents also inhibit tubulin polymerization. Combretastatins, as exemplified by combretastatin A-4 (CA4[a]) and its phosphorylated prodrug combretastatin A-4 phosphate (CA4P), are a class of drugs that are in clinical trials as antitumor agents that bind to the colchicine site.[1] Colchicine itself is not used as an antitumor agent but is used in the treatment of gout and familial Mediterranean fever. There are no clinically approved antitumor agents that bind to the colchicine site. However, several of these agents are currrently in clinical trials,[6,7] demonstrating the importance of developing colchicine site agents both for use alone and in combination chemotherapy protocols.

Half of all human tumors have mutations in the p53 gene, and the most effective drugs in p53 mutant cell lines are tubulin-binding agents.[8] This further emphasizes the importance of developing new tubulin-binding drugs that are active against resistant tumors. Comprehensive reviews of structures and activities for these agents are available in the literature.[9−13]

Despite the unprecedented success of microtubule disrupting agents in cancer chemotherapy, multidrug resistance (MDR) is a major limitation of cancer chemotherapy, and MDR tumors are usually resistant to tubulin-binding drugs. Overexpression of P-glycoprotein (Pgp) has been reported in the clinical setting in a number of tumor types, particularly after patients have received chemotherapy.[11,12] In addition, it has also been reported that Pgp expression may be a prognostic indicator in certain cancers and is associated with poor response to chemotherapy,[13,14] demonstrating the clinical importance of this mechanism of tumor resistance. Overexpression of Pgp appears to be more relevant in the clinical setting than elevation of MRP1 levels.[15] The overwhelming

*To whom correspondence should be addressed. (A.G.) Telephone: 412-396-6070. Fax 412-396-5593. E-mail gangjee@duq.edu. (S.L.M.) Telephone 210-567-4788. Fax 210-567-4300. E-mail mooberry@uthscsa.edu.

[a]Abbreviations: Combretastatin A-4, CA4; multiple drug resistance, MDR; P-glycoprotein, Pgp; multidrug resistance protein 1, MRP1; receptor tyrosine kinase, RTK; epidermal growth factor receptor, EGFR; platelet-derived growth factor receptor, PDGFR; vascular endothelial growth factor receptor, VEGFR; relative resistance, Rr; *N*-deacetyl-*N*-(2-mercaptoacetyl)colchicine, DAMA colchicine; 2-methoxyestradiol, 2ME2.

 Published on Web 10/25/2010

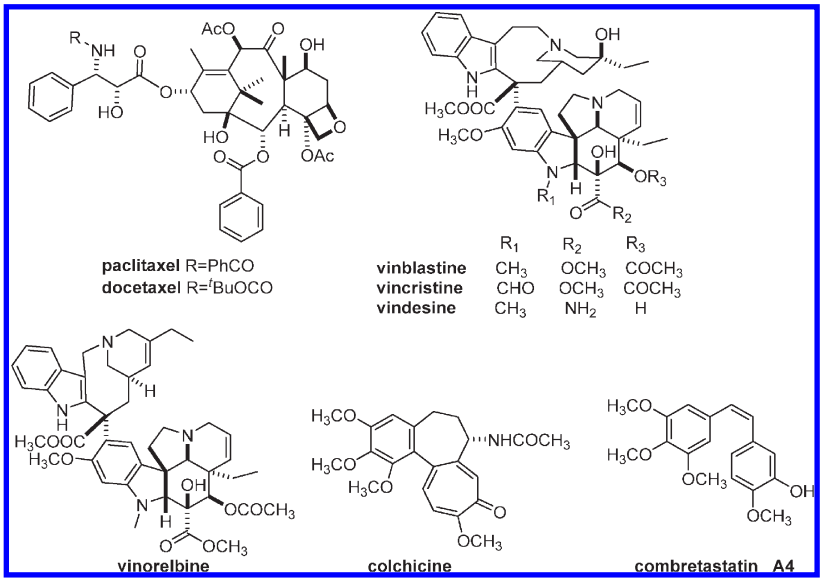

Figure 1. Structures of microtubule targeting agents.

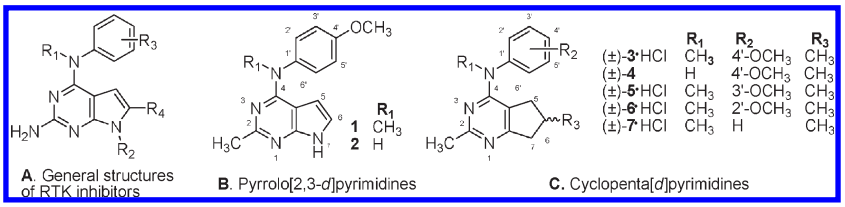

Figure 2. Lead compounds.

lack of success of Pgp inhibitors in the clinic indicates that the ability to overcome to Pgp-mediated resistance is an important property for new microtubule targeting agents.[12,16] Such agents will fill an unmet need in the clinic for patients that develop resistance due to Pgp overexpression.

The other clinical mechanism of resistance to microtubule targeted agents involves the expression of specific isotypes of β-tubulin, of which the βIII-tubulin isotype is of paramount concern. There is unequivocal clinical evidence that βIII-tubulin expression is involved in resistance to taxoids and vinca alkaloids in multiple tumor types including non-small cell lung,[17−19] breast,[20] and ovarian cancers.[21,22] Excellent reviews of the importance of βIII-tubulin in tumor resistance to microtubule targeted agents are available.[23] In a recent study, Stengel et al.[24] and Lee et al.[25] have shown that colchicine site agents circumvent βIII-tubulin resistance and highlight the critical importance of developing new agents that bind to the colchicine site as an alternative to the taxoids for the treatment of refractory cancers. The ability to overcome resistance due to Pgp and βIII-tubulin expression was part of the impetus for the recent FDA approval of ixabepilone as an antitumor agent and further attests to the importance of developing agents that overcome these resistance mechanisms.[26]

An additional serious problem with several of the currently used antitubulin agents, particularly the taxoids, is their poor water solubility. This necessitates their formulation in polyoxyethylated castor oil or polysorbate, which can cause hypersensitivity reactions and require long administration times. This is a problem, too, with ixabepilone, which also needs to be dissolved in polyoxyethylated castor oil. Thus water-soluble microtubule targeted agents are highly coveted, and an enormous effort continues to chemically modify and/or formulate analogues of these agents to increase their water solubility.

Synergistic or additive effects of microtubule targeted agents used in combination occurs, in part, due to the different target sites of the agents on tubulin. Estramustine and paclitaxel, which bind to different sites on tubulin, can act synergistically or additively in combination.[27] Combinations including paclitaxel or docetaxel plus vinorelbine are more efficacious in combination than as single agents.[28,29] CA4P is currently in clinical trials in combination with paclitaxel (www.clinicaltrials.gov).[29] As noted above, no colchicine site agent is FDA approved for cancer chemotherapy. There are however several colchicine site agents in clinical trials, and approval of such a drug would allow evaluation of whether enhanced activity could be obtained by combining it with a taxoid or vinca alkaloid. Thus, new tubulin-binding agents that do not act at the taxoid or vinca alkaloid site on tubulin are of considerable interest, both as single agents and to combine with these established drugs.

Synthesis of Water-Soluble Microtubule Targeting Agents

We had previously synthesized 2-amino-4-anilino-6-substituted pyrrolo[2,3-*d*]pyrimidines as receptor tyrosine kinase (RTK) inhibitors of general structure **A** (Figure 2). Three possible binding modes to RTK were suggested from molecular modeling. To define the mode(s) of binding, we synthesized the aniline N-methylated analogue (**A**; $R_1 = CH_3$; $R_2 = H$), the N7-methylated analogue (**A**; $R_1 = H$; $R_2 = CH_3$), and the aniline N- and N7-dimethylated analogue (**A**; $R_1 = CH_3$; $R_2 = CH_3$). These results were first reported in 2005.[30,31] Further, analogue design from these lead compounds afforded the pyrrolo[2,3-*d*]pyrimidines **1**−**2** and the cyclopenta[*d*]pyrimidine (±)-**3** (Figure 2) as the free base, and **1**−(±)-**3** as the HCl, water-soluble salts as well. Compounds **1**−(±)-**3** were not RTK

inhibitors (evaluated against EGFR, VEGFR-1, VEGFR-2, and PDGFR-β), but in the preclinical screening program of the National Cancer Institute in its 60 tumor cell line panel **1** inhibited the proliferation of most of the 60 cancer cell lines with a GI_{50} of less than 500 nM (Table 1) and (±)-**3**·HCl inhibited the proliferation of the majority of the 60 cell lines with a potent GI_{50} of less than 30 nM (Table 1).

The potent activities of these compounds prompted a COMPARE analysis,[32,34] which showed vincristine sulfate to have the closest Pearsons correlation coefficient with **1** and (±)-**3**·HCl. Other compounds, such as vinblastine sulfate and maytansine, also tubulin binding agents, were ranked as the next closest correlation. This clearly warranted the evaluation of **1** and (±)-**3**·HCl as tubulin binding agents. It was also of interest to synthesize and evaluate **2**, the desmethyl analogue of **1**, and (±)-**4**, the desmethyl analogue of (±)-**3**. In addition, due to the more potent activity of (±)-**3**·HCl in the NCI preclinical panel as compared to **1**, compounds (±)-**5**·HCl−(±)-**7**·HCl (Figure 2) were also synthesized to determine the position and importance of the 4′-OMe moiety to the biological activity of (±)-**3**·HCl.

Chemistry

Compound **1** was synthesized as shown in Scheme 1. Ethyl 2-cyano-4,4-diethoxybutanoate **8** and acetamidine·HCl, **9**, were reacted at reflux for 5 h and cooled to 0 °C, and then the precipitate was collected and treated with conc. H_2SO_4 in ethanol at reflux for 2 h to afford 2-methyl-4-oxo-pyrrolo[2,3-*d*]pyrimidine **10** in 64% yield. Chlorination with $POCl_3$ afforded **11** (83% yield).[35] Treatment of **11** with the appropriate anilines **12** afforded **1** (R = CH_3) (80% yield) and **2** (R = H) (41%). The water-soluble hydrochloride salt of **1** was obtained as a white precipitate (~100%) by dissolving **1** in anhydrous ether followed by bubbling anhydrous HCl gas.

Target compounds (±)-**3**−(±)-**7** were prepared as shown in Scheme 2. 2,6-Dimethyl-6,7-dihydro-3*H*-cyclopenta[*d*]pyrimidin-4(5*H*)-one (±)-**14** was prepared via the reaction of commercially available 3-methyladipic acid (±)-**13** and conc. H_2SO_4 at reflux in ethanol and a Dieckmann condensation in the presence of elemental sodium in toluene, followed by treatment with acetamidine·HCl **9** (21% over three steps). Chlorination of (±)-**14** with $POCl_3$ for 3 h at reflux afforded (±)-**15** (69%).[36] Compound (±)-**15** was unstable and easily decomposed to (±)-**14** if not used immediately. Reaction of (±)-**15** with the appropriate anilines in *i*-PrOH in the presence of 2−3 drops of conc. HCl afforded (±)-**3**−(±)-**7**. Anhydrous HCl gas was bubbled through an anhydrous ether solution of (±)-**3**, (±)-**5**−(±)-**7** to afford the corresponding HCl salts as white solids.

Biological Evaluations

NCI Cytotoxicity Studies and Antimicrotubule Effects in Cells. Compounds **1** and (±)-**3**·HCl showed potent GI_{50}'s in most of the NCI 60 cancer cell lines (Table 1). The microtubule disrupting effects of **1** and (±)-**3**·HCl were observed (Figure 3) in a cell-based phenotypic screen. Compounds **1** and (±)-**3**·HCl caused dramatic reorganization of the interphase microtubule network, similar to the effects of colchicine and CA4P. The EC_{50} (concentration required to cause 50% loss of cellular microtubules) (Table 2) was calculated to be 7 nM for CA4P,[25] 56 nM for (±)-**3**·HCl, and 5.8 μM for **1**. Consistent with effects on cellular microtubules,

Table 1. Tumor Cell Growth Inhibitory Activity GI_{50} (nM) of **1** and (±)-**3**·HCl in NCI 60 Cell Line Panel

panel/cell line	GI_{50} (nM) compound **1**	GI_{50} (nM) compound (±)-**3**·HCl
Leukemia		
CCRF-CEM	315	16.3
HL-60(TB)	190	< 10
K-562	179	< 10
MOLT-4	503	31.8
RPMI-8226		15.7
SR	87.6	< 10
NSCLC		
A549/ATCC	723	24.4
EKVX	875	19.6
HOP-62	291	19.4
HOP-92	4800	55.4
NCI-H226	623	31.5
NCI-H23	438	16.4
NCI-H322M	428	59.0
NCI-H460	351	23.4
NCI-H522	40.2	< 10
Colon Cancer		
COLO 205	243	18.3
HCC-2998	271	24.0
HCT-116	344	15.1
HCT-15	275	< 10
HT29	279	11.8
KM12	181	< 10
SW-620	246	< 10
CNS Cancer		
SF-268	449	15.2
SF-295	269	< 10
SF-539	288	11.4
SNB-19	612	36.9
SNB-75	185	< 10
U251	440	12.5
Melanoma		
LOX IMVI	407	22.7
M14	218	10.2
MDA-MB-435	44.2	< 10
SK-MEL-2	251	33.1
SK-MEL-28	603	< 10
SK-MEL-5	177	< 10
UACC-62	625	< 10
Ovarian Cancer		
IGROVI	340	11.0
OVCAR-3	192	< 10
OVCAR-4	7730	26.8
OVCAR-5	1670	38.5
OVCAR-8	639	32.8
NCI/ADR-RES	164	< 10
SK-OV-3	248	27.5
Renal Cancer		
786 - 0	433	34.8
A498	198	< 10
ACHN	556	14.6
CAKI-1	339	
RXF 393	226	< 10
SN12C	854	31.8
TK10	390	292
UO-31	307	13.4
Prostate Cancer		
PC-3	509	14.6
DU-145	269	21.4
Breast Cancer		
MCF7	314	< 10
MDA-MB-231/ATCC	1260	24.6
HS 578T	249	< 10
BT-549		21.9
MDA-MB-468	208	< 10

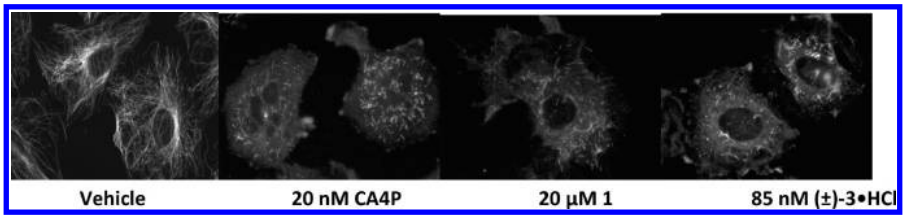

Figure 3. Effects of CA4P, **1**, and (±)-**3**·HCl on interphase microtubules. A-10 cells were treated with vehicle or compounds as indicated for 18 h, and then the cells were fixed and microtubules visualized by indirect immunofluorescence techniques.

Scheme 1. Synthesis of Pyrrolo[2,3-*d*]pyrimidines **1** and **2**[a]

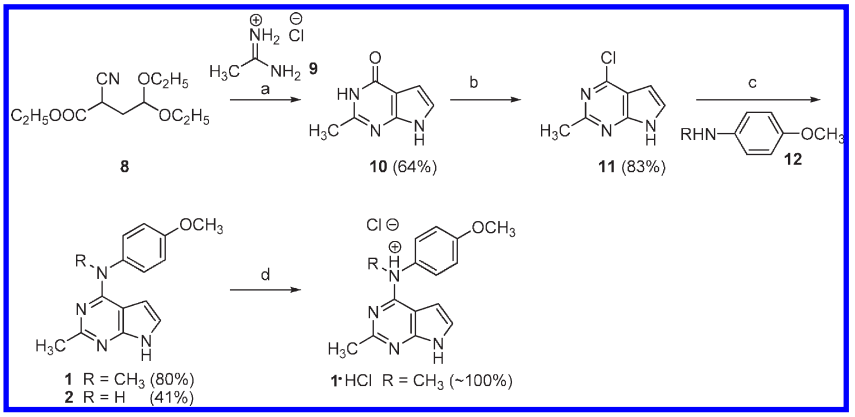

[a] Reagents and conditions: (a) (i) 2-bromo-1,1-diethoxyethane, NaOMe, anhyd. DMF, 90 °C, 4 h; (ii) acetamidine·HCl, NaOEt, EtOH, reflux, 3 h; (iii) conc. H_2SO_4, EtOH, reflux, 2 h. (b) $POCl_3$, reflux, 3 h. (c) *i*-PrOH, HCl (1 drop), reflux, 4 h. (d) Anhyd. HCl gas, anhyd. ether.

Scheme 2. Synthesis of Cyclopenta[*d*]pyrimidines (±)-3 − (±)-7 and Their HCl Salts[a]

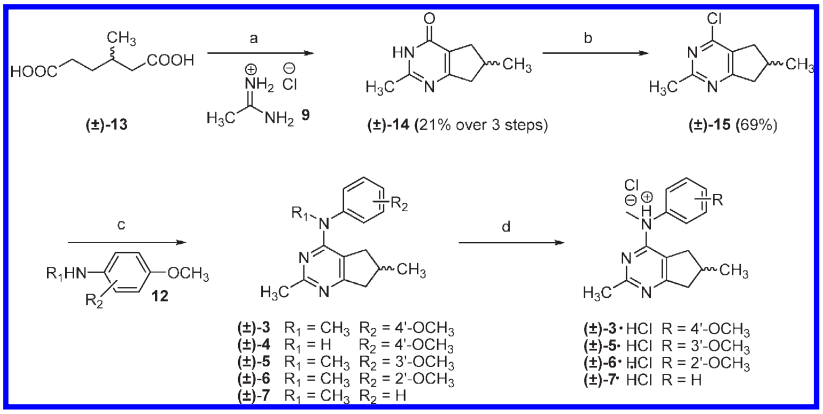

[a] Reagents and conditions: (a) (i) conc. H_2SO_4, EtOH, reflux, 8 h; (ii) Na, toluene, reflux, 3 h; (iii) acetamidine·HCl **9**, *t*-BuOK, *t*-BuOH. (b) $POCl_3$, reflux, 3 h. (c) *i*-PrOH, HCl (2−3 drops), reflux, 3−6 h. (d) Anhyd. HCl gas, anhyd. ether.

Table 2. IC_{50} Values for Inhibition of Proliferation of MDA-MB-435 Cells and EC_{50}s for Cellular Microtubule Loss

compound	$IC_{50} \pm SD$ (MDA-MB-435)	EC_{50} for microtubule depolymerization
1	183 ± 3.4 nM	5.8 μM
2	> 10 μM	> 40 μM
(±)-**3**·HCl	17.0 ± 0.7 nM	56 nM
(±)-**4**	> 10 μM	> 40 μM
(±)-**5**·HCl	153 ± 11.1 nM	3.0 μM
(±)-**6**·HCl	ND[a]	> 40 μM
(±)-**7**·HCl	2.7 ± 0.3 μM	> 40 μM

[a] ND: Not determined.

1 and (±)-**3**·HCl caused the formation of aberrant mitotic spindles and mitotic accumulation when measured by flow cytometry (Figure 4). Compounds **1** and (±)-**3**·HCl are potent microtubule depolymerizers in cells, confirming the COMPARE analysis results.

Antiproliferative Effects. Compounds **1** and (±)-**3**·HCl were tested for antiproliferative effects against the drug sensitive MDA-MB-435 cell line using the sulforhodamine B assay (SRB assay).[37,38] The data (Table 2) indicate that (±)-**3**·HCl has potent antiproliferative effects with an IC_{50} (concentration required to cause 50% inhibition of proliferation) of 17.0 ± 0.7 nM. Compound **1** is less potent, consistent with its effects in the phenotypic assay and by flow cytometry, with an IC_{50} of 183 ± 3.4 nM.

The ability of **1** and (±)-**3**·HCl to circumvent Pgp-mediated drug resistance was evaluated by using an SK-OV-3 isogenic cell line pair (Table 3). In this cell line pair, the relative resistance (Rr) of paclitaxel, a well-known Pgp substrate, is greater than

800 while Rr values of 1.2 and 1.6 were obtained with **1** and (±)-**3**·HCl, respectively, consistent with the Rr values obtained with other colchicine site agents, CA4P and 2ME2 of 1.5−2.6. These data suggest that both **1** and (±)-**3**·HCl are poor substrates for transport by Pgp and thus have advantages over some clinically useful tubulin-targeting drugs such as paclitaxel.

A second mechanism of drug resistance that can lead to treatment failure with tubulin-targeting drugs is the expression of the βIII isotype of tubulin as discussed above. An isogenic HeLa cell line pair was used to evaluate the effect of βIII tubulin expression on the activities of **1** and (±)-**3**·HCl.[39] Compounds **1** and (±)-**3**·HCl have Rr values of 0.6−0.7 (Table 3) in this cell line pair, suggesting that they overcome drug resistance mediated by βIII tubulin as compared with paclitaxel, which has a Rr of 4.7. Thus, both **1** and (±)-**3**·HCl inhibit tumor cells with equal potency without regard to their expression of Pgp or βIII-tubulin.

Further Mechanistic Studies. Studies were conducted to determine if **1** and (±)-**3**·HCl inhibited the polymerization of purified bovine brain tubulin, as would be predicted from the effects in cells. These biochemical studies provide an indication of a direct interaction of the compounds with tubulin.

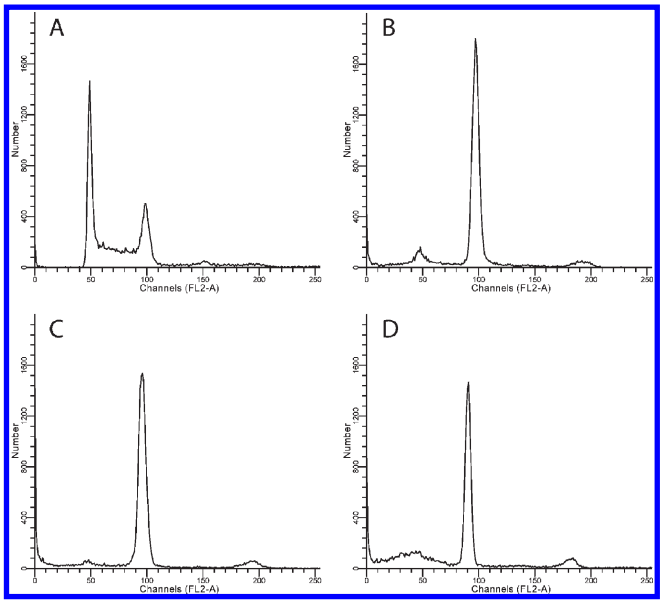

Figure 4. Cell cycle distribution. MBA-MB-435 cells were treated with vehicle (A), 12.5 nM paclitaxel (B), 45 nM (±)-**3**·HCl (C), or 850 nM **1** (D) for 24 h. The cells were then harvested, stained with propidium iodide, and evaluated by flow cytometry.

An initial study, shown in Figure 5, indicates that both **1** and (±)-**3**·HCl are potent inhibitors of purified tubulin assembly. Both compounds were therefore compared with CA4P as inhibitors of assembly in a quantitative study (Table 4). In this assay, both **1** and (±)-**3**·HCl inhibited tubulin assembly about as well as CA4 (Table 4). The data in Table 4 also show that **1** and (±)-**3**·HCl bind at the colchicine site on tubulin, since they inhibited [^{3}H]colchicine binding to the protein, although not as potently as CA4.

To determine the structural requirements for the 4′-OCH_3 and N4-CH_3 moieties for activity, compounds **2** and (±)-**4**−(±)-**7** were synthesized. The superior activity of (±)-**3**·HCl suggests that the pyrrole NH of **1** is not important for activity. Table 2 indicates that the methylation of the aniline N is crucial for activity in both scaffolds (compare **1** with **2** and (±)-**3**·HCl with (±)-**4**). In addition, the 4′-OCH_3 moiety is important for potent activity (compare (±)-**3**·HCl with (±)-**7**·HCl), and the optimum location for the methoxyl group is at the 4′-position since (±)-**5**·HCl, which has a 3′-OCH_3, was about 9-fold less potent than (±)-**3**·HCl, which has a 4′-OCH_3. Finally, (±)-**6**·HCl, the analogue with a 2′-OCH_3, was inactive.

Molecular Modeling

In an attempt to explain the molecular basis of the potent activity of the *N*-Me analogues **1** and (±)-**3**·HCl and the inactivity of the N-desmethyl analogues **2** and (±)-**4**, we modeled compounds **1**−**7** into the colchicine site. The X-ray crystal structure of tubulin at 3.58 Å resolution was obtained from the protein database (PDB ID 1SA0[40]). This crystal structure contains the αβ dimers of tubulin complexed with *N*-deacetyl-*N*-(2-mercaptoacetyl)colchicine (DAMA colchicine), a close structural analogue of colchicine. The binding of colchicine to the tubulin dimer has been described in the literature.[40−42] Colchicine binds to β-tubulin at its interface with α-tubulin. The colchicine site has dimensions of ∼10 Å × ∼10 Å × ∼4−5 Å and is composed of strands S8 and S9, loop T7, and helices H7 and H8 (nomenclature and amino acid residue positions as described in ref 40) from the β subunit and loop T5 from the α subunit of tubulin. Thrα179 and Valα181 in the α-tubulin subunit form hydrogen bonds with colchicine. Additionally, Cysβ241 forms a hydrogen bond with the oxygen atom of the 3-OCH_3 in the A-ring of colchicine. Further hydrophobic stabilization is afforded by side chain atoms of Valα181 and Metβ259. In addition, the carbonyl group of the A-ring H-bonds with Lysβ352.[41,42]

Docking of (*R*)-3. Docking studies were performed using the docking suite of Molecular Operating Environment software (MOE 2008.10).[43] Details of the docking protocol

Table 3. **1** and (±)-**3**·HCl Circumvent Pgp and βIII-Tubulin Mediated Resistance[a]

	effect of Pgp on drug sensitivity[b]			effect of βIII-tubulin on drug sensitivity[c]		
	IC_{50} ± SD (nM)			IC_{50} ± SD (nM)		
drug	SK-OV-3	SK-OV-3 MDR-1-6/6	Rr	HeLa	WT βIII	Rr
paclitaxel	3.0 ± 0.06	2600 ± 270	864	1.6 ± 0.2	7.7 ± 0.2	4.7
CA4P	4.5 ± 0.2	6.6 ± 1.3	1.5	4.7 ± 0.2	5.7 ± 0.4	1.2
2ME2	867 ± 36	2268 ± 235	2.6	608 ± 55	586 ± 37	1
1	278 ± 19	435 ± 33	1.6	270 ± 21	186 ± 17	0.7
(±)-**3**·HCl	38.6 ± 3.1	44.4 ± 3.2	1.2	37.3 ± 4.1	23.9 ± 1.7	0.6

[a] Rr: Relative resistance. [b] Antiproliferative effects of (±)-**3**·HCl and **1** in parental and *MDR-1*-transducted cell lines in comparison with other microtubule disrupting agents. The IC_{50} values were determined using the SRB assay ($n = 3 \pm SD$). The Rr was calculated by dividing the IC_{50} of the Pgp overexpressing cell line by the IC_{50} of the parental cell line. [c] Effects of the expression of βIII-tubulin on the sensitivity of cell lines to microtubule-targeting agents. The Rr was calculated by dividing the IC_{50} of the WT βIII cell line by the IC_{50} of the parental HeLa cells.

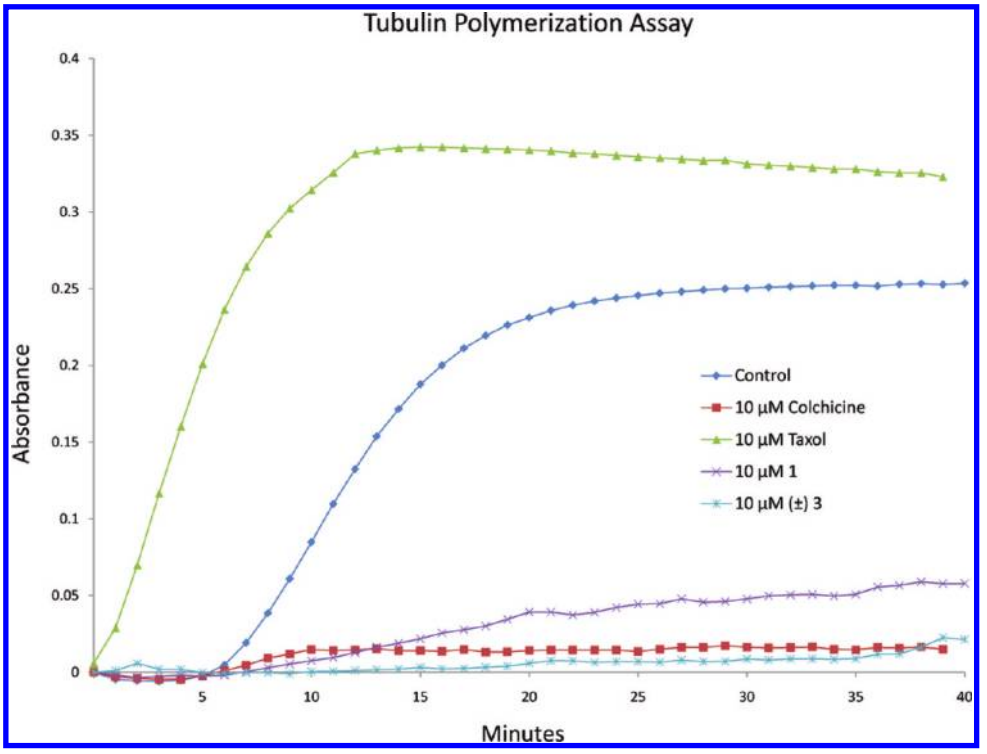

Figure 5. Effects of microtubule disrupting agents on tubulin polymerization. Paclitaxel represents a positive control for a microtubule stabilizer and colchicine the control for a microtubule depolymerizer. The assays were conducted using purified bovine brain tubulin from Cytoskeleton Inc. in the presence of 10% glycerol, 3 mg/mL purified tubulin, and 10 mM GTP.

Table 4. Inhibition of Tubulin Assembly and Inhibition of Colchicine Binding

	inhibition of tubulin assembly	inhibition of colchicine binding	
		% Inhibition ± SD	
cmpd	IC_{50} ± SD (nM)	1 μM	5 μM
CA4	1.0 ± 0.09	88 ± 2	99 ± 0.2
1	2.6 ± 0.05	ND[a]	70 ± 2
(±)-**3**·HCl	1.9 ± 0.01	60 ± 2	84 ± 3

[a] ND: Not determined.

used are provided in the Experimental Section. Multiple low-energy conformations (within 1 kcal/mol of the best pose) were obtained on docking (*R*)-**3** and other analogues. The multiple docked poses can be explained by the large volume of the active site (10 Å × 10 Å × 4−5 Å).[41] Figure 6 shows the docked conformation of (*R*)-**3** which was arbitrarily selected as a working model for the docking of compounds **1**−**7** on the basis of their structural similarity to the bound conformation of DAMA colchicine. The pose in Figure 6 for (*R*)-**3** had a score (−6.8379 kcal/mol) within 1 kcal/mol of the best scored pose. Comparison of the docked conformation of (*R*)-**3** with the crystal structure conformation of DAMA colchicine shows overlap of the 4′-OCH_3 phenyl group of (*R*)-**3** with the trimethoxybenzene A-ring of DAMA colchicine (Figure 6). In this pose, the 4′-OCH_3 of (*R*)-**3** overlaps with the 3′-OCH_3 group in the A ring of DAMA colchicine. Similar interactions of the $-OCH_3$ groups with Cysβ241 have been reported in the literature.[41,44] The conformation of (*R*)-**3** depicted in Figure 6 permits the formation of a hydrogen bond between Cysβ241 and the oxygen atom of the 4′-OCH_3 of (*R*)-**3** as is observed between Cysβ241 and the 3′-OCH_3 group of DAMA colchicine in its X-ray crystal structure with tubulin. The phenyl ring of (*R*)-**3** mimics the A ring of colchicine and is involved in hydrophobic interactions with amino acids from β-tubulin (Leuβ248, Alaβ250, Leuβ255, and Alaβ316). Additionally, the methyl group of the 4′-OCH_3 moiety could interact with the side chain of Ileβ378 and/or with the side chain of Valβ318.

We[45−49] and others[50] have previously demonstrated that similar CH_3 moieties dictate the biological activities predicated on hydrophobic interactions and/or conformational restriction. It was of interest to extend these findings to provide a rationale for the high potency of the *N*-CH_3 analogues of the present study compared with the *N*-desmethyl analogues.

The *N*-CH_3 group of (*R*)-**3** occupies a region in space in proximity to the C5 and C6 atoms of the B-ring of DAMA colchicine. In this orientation, the *N*-CH_3 group is involved in hydrophobic interactions with the side chain C atoms of Lysβ254 and Alaβ250. An additional hydrophobic interaction between the *N*-CH_3 moiety of (*R*)-**3** and the side chain C-atom of Leuβ248 also occurs due to the flexible nature of the protein (measured distance between *N*-CH_3 and side chain C of Leuβ248 is 4.21 Å). These interactions could assist in stabilization of the docked conformation of (*R*)-**3** and could explain, in part, the observed difference in activity of the *N*-desmethyl analogue, (*R*)-**4**, which would lack these additional interactions (Figure 7). The *N*-CH_3 also aids in maintaining the relative conformations of the cyclopenta-[*d*]pyrimidine and the phenyl ring. While similar docked poses were observed for (*R*)-**4**, the docked poses of compounds with the *N*-CH_3 group consistently scored higher (∼1 kcal/mol) than those of compounds that lack the *N*-CH_3 group.

A systematic conformational search carried out using Sybyl X 1.1[51] for energy minimized structures of (*R*)-**3** and

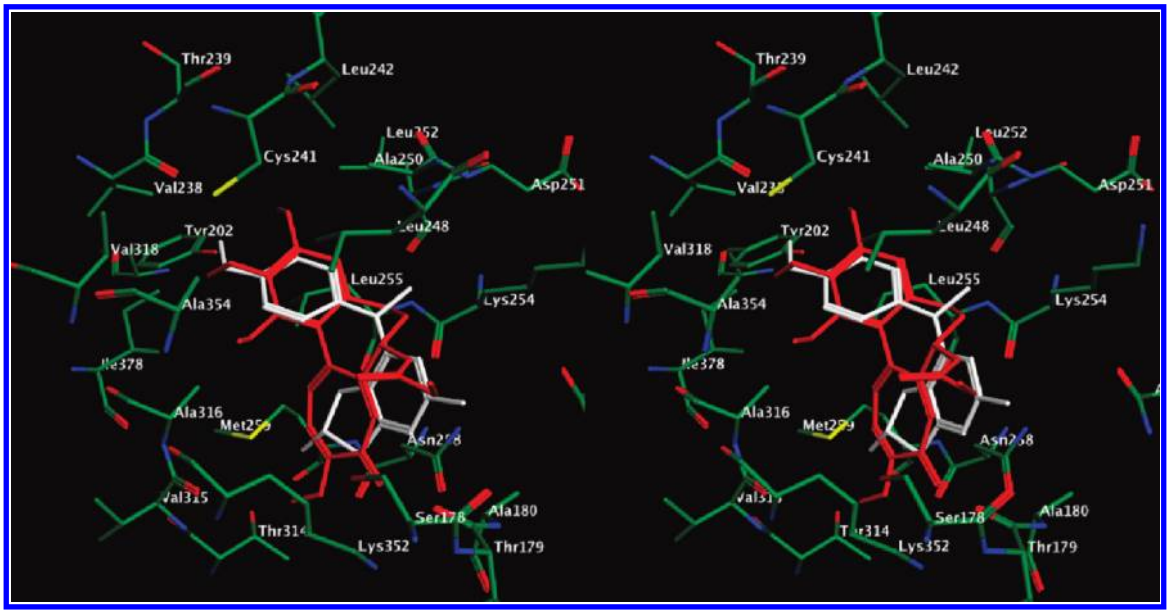

Figure 6. Stereo view. Docked pose of (*R*)-**3** (white) overlaid with DAMA colchicine (red) in the colchicine site of tubulin.

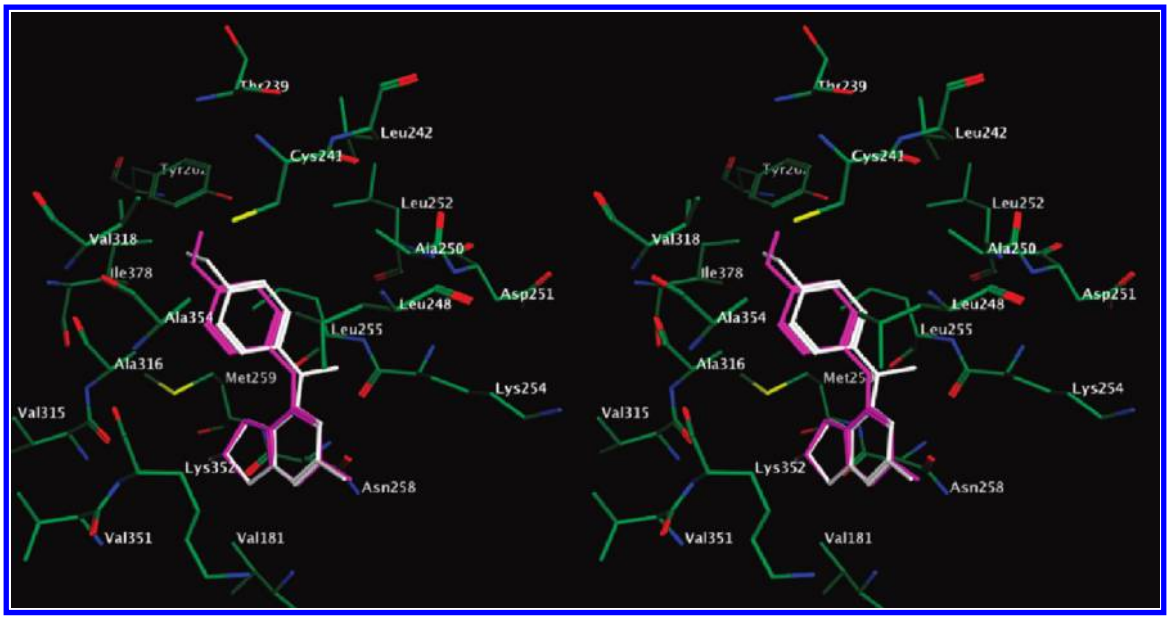

Figure 7. Stereo view. Superimposition of the docked poses of (*R*)-**3** (white) and (*R*)-**4** (magenta) in the colchicine site of tubulin.

(*R*)-**4** returned a lower number of conformers for the *N*-CH_3 compound (*R*)-**3** compared with the NH compound (*R*)-**4** using the same settings. This is indicative of restrictions on the rotational freedom of the 4′-OCH_3 phenyl ring of (*R*)-**3** in the presence of the *N*-CH_3 moiety and decreases the number of low energy conformations of the 4′-OCH_3 phenyl ring relative to the cyclopenta[*d*]pyrimidine scaffold of (*R*)-**3**. Similar results were obtained for the conformational search of **1** and **2**.

The cyclopenta[*d*]pyrimidine of (*R*)-**3** ring partially overlaps with the C-ring of DAMA colchicine and is stabilized by hydrophobic interactions with side chain C atoms of Leuβ255, Asnβ258, and Lysβ252. The C7 of (*R*)-**3** overlaps the C9 carbonyl C of DAMA colchicine. The C2-CH_3 moiety of (*R*)-**3** is involved in a hydrophobic interaction with Alaα180 (4.35 Å), while the C6-CH_3 group of (*R*)-**3** is involved in hydrophobic interactions with Valα181 and Alaβ316. We did not observe a significant difference in the binding poses and docked scores of (*R*)-**3** (−6.8379 kcal/mol) and (*S*)-**3** (−6.9454 kcal/mol) due to the chirality of the C6-CH_3 group (Figure 8). Whether this slight predicted difference between the two isomers is reflected in the biological activities can only be determined once the two isomers are individually synthesized and evaluated.

While this work was in progress, studies describing a series of quinazolines[51−54] and thieno[3,2-*d*]pyrimidines[55] as potent apoptosis inducers were published. These reports suggest a similar function for the *N*-CH_3 moiety, but do not provide molecular details about the binding modes of the quinazolines and/or thieno[3,2-*d*]pyrimidines to tubulin.

Molecular modeling suggests that the binding interactions afforded by the 4′-OCH_3 group on the anilino ring play an important part and dictate the potency of these compounds against tubulin, since deletion or moving the 4′-OCH_3 moiety results in a significant loss of activity. However, molecular modeling does not provide a reason(s) for the loss of potency of

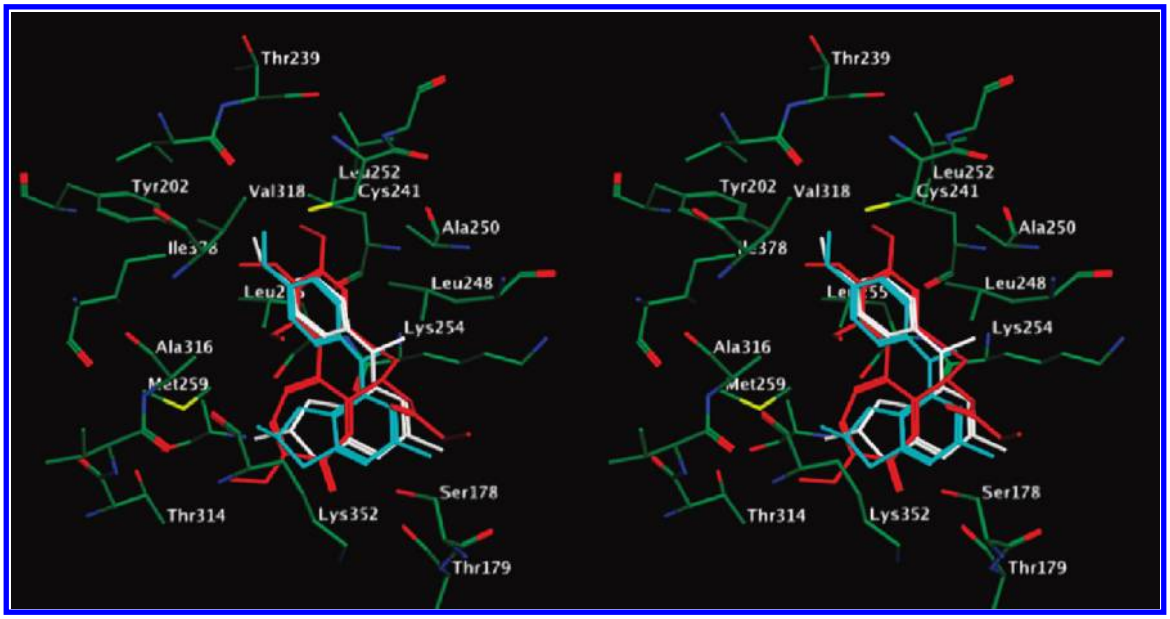

Figure 8. Stereo view. Superimposition of the docked poses of (*R*)-**3** (white), (*S*)-**3** (cyan), and DAMA colchicine (red) in the colchicine site of tubulin.

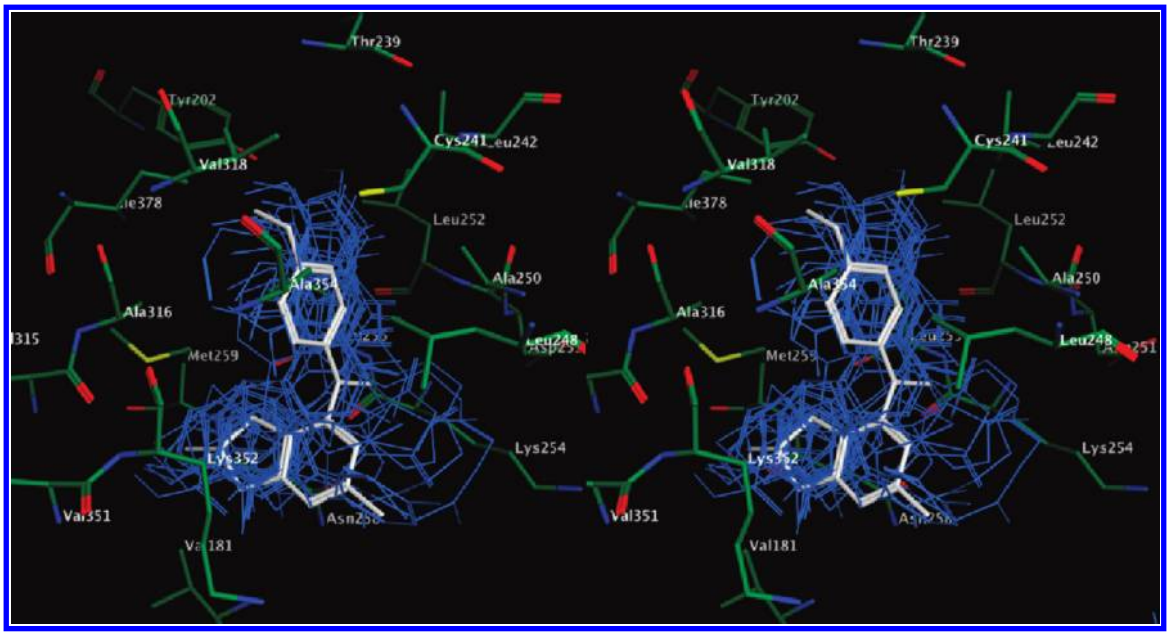

Figure 9. Stereo view. Docking mode of (*R*)-**3** (white) overlaid with docked poses of 15 ligands[41] (blue) in the colchicine site of tubulin.

(±)-**6** (2′-OCH_3) compared with (±)-**3**. We speculate that the loss of potency could be explained by the loss of interactions of the 4′-OCH_3 moiety of (±)-**3** and/or the additional conformational restriction of the anilino ring by a combination of *N*-methylation and the 2′-OCH_3 moiety on the phenyl ring or both.

The docking mode of **1** (not shown) was strikingly similar to the docking mode of (*R*)-**3**. The pyrrole NH of **1** was not involved in a hydrogen bond with the amino acid residues of the tubulin binding site. Additionally, **1** lacks the 6-CH_3 substitution in (*R*)-**3** and could thus lack the additional bonding afforded by the substituent at C6. The docked pose of **1** had a score of −6.0330 kcal/mol, somewhat less but comparable to that of (*R*)- and (*S*)-**3**.

We also compared the binding mode of compounds **1**−**7** to the proposed binding modes[41] of 15 known tubulin inhibitors. As an example, (*R*)-**3** retains the key binding interactions exhibited by the known tubulin inhibitors and is in a conformation consistent with those for the reported compounds[41] (Figure 9). Similar docked poses were observed in this study for compounds **1**−**7**.

In summary, we report the synthesis and identification of the mechanism of action of water-soluble, colchicine site microtubule depolymerizing agents **1** and (±)-**3**·HCl. These compounds inhibit the growth of tumor cells with GI_{50} values in the nanomolar range and overcome two clinically important tumor resistance mechanisms that limit activity of microtubule targeting agents, expression of Pgp and βIII tubulin. For these analogues, the 6-CH_3 cyclopenta[*d*]pyrimidine scaffold is better than the pyrrolo[2,3-*d*]pyrimidine scaffold, and both the 4-*N*-methyl and 4′-OCH_3 groups on the aniline ring are required for optimal potency. We have also

provided an explanation of the importance of the N-CH_3 moiety of **1** and (±)-**3**·HCl for biological activity via molecular modeling. Compounds **1** and (±)-**3**·HCl are important lead analogues for the development of further compounds for in vivo evaluation and possible advancement into clinical trials.

Experimental Section

Analytical samples were dried in vacuo (0.2 mmHg) in a CHEM-DRY drying apparatus over P_2O_5 at 50 °C. Melting points were determined on a digital MEL-TEMP II melting point apparatus with a FLUKE 51 K/J electronic thermometer, and are uncorrected. Nuclear magnetic resonance spectra for proton (^{1}H NMR) were recorded on Bruker Avance II 400 (400 MHz) and 500 (500 MHz) NMR systems. The chemical shift values are expressed in ppm (parts per million) relative to tetramethylsilane as an internal standard: s, singlet; d, doublet; t, triplet; q, quartet; m, multiplet; br, broad singlet. Thin-layer chromatography (TLC) was performed on Whatman Sil G/UV254 silica gel plates with a fluorescent indicator, and the spots were visualized under 254 and 366 nm illumination. Proportions of solvents used for TLC are by volume. Column chromatography was performed on a 230−400 mesh silica gel (Fisher Scientific) column. Elemental analyses were performed by Atlantic Microlab, Inc., Norcross, GA. Element compositions are within ±0.4% of the calculated values and indicate >95% purity. Fractional moles of water or organic solvents frequently found in some analytical samples could not be prevented despite 24−48 h of drying in vacuo and were confirmed where possible by their presence in the ^{1}H NMR spectra. Mass spectrum data were acquired on the Agilent G6220AA TOF LC/MS system using the nano ESI (Agilent chip tube system with infusion chip). All solvents and chemicals were purchased from Sigma-Aldrich Co. or Fisher Scientific Inc. and were used as received.

2-Methyl-3*H*-pyrrolo[2,3-*d*]pyrimidin-4(7*H*)-one (10). The synthesis of **10** utilized a reported method.[35] To a solution of ethyl 2-cyanoacetate **8** (10 mmol, 1.13 g) in anhydrous dimethylformamide (DMF, 20 mL) was added sodium methoxide (10 mmol, 0.54 g). After stirring for 30 min, 2-bromo-1,1-diethoxyethane (10 mmol, 1.97 g) was added, and the reaction was heated at 90 °C for 4 h. After cooling to room temperature, the reaction solution was extracted with diethyl ether (2 × 20 mL). The ether layer was collected, dried over sodium sulfate, and evaporated to give a pale yellow liquid. The liquid was added to a solution of acetamidine hydrochloride **9** (10 mmol, 0.94 g) and sodium ethoxide (10 mmol, 0.68 g) in ethanol (20 mL) and refluxed for 3 h. The solution was evaporated to dryness and extracted with ethyl acetate and water. The organic layer was collected and evaporated to afford a solid. Concentrated sulfuric acid (2 mL) in ethanol (10 mL) was added to the solid, and the mixture was kept at reflux for 2 h. At the end of the reaction, water (10 mL) was added and the pH was adjusted to 8 using ammonium hydroxide. The precipitate obtained was collected and dried to give **10** as an off-white powder (0.85 g). Compound **10** was used without further purification.

4-Chloro-2-methyl-7*H*-pyrrolo[2,3-*d*]pyrimidine (11). Compound **10** (5 mmol, 0.75 g) was treated with $POCl_3$ (10 mL) and heated under reflux for 3 h, and the remaining $POCl_3$ was removed in vacuo. Ammonium hydroxide was carefully added to the resulting slurry, followed by extraction with ethyl acetate. After combining the organic phases and evaporation, compound **11** was obtained as a pale yellow powder (0.67 g, 81%) and used without further purification. R_f 0.45 (CH_3OH:$CHCl_3$ = 1:5). An analytical sample was purified for ^{1}H NMR (DMSO-d_6): δ 2.28 (s, 3 H, 2-CH_3), 6.35 (d, 1 H, 5-H, J = 3.28 Hz), 6.93 (d, 1 H, 6-H, J = 3.28 Hz), 11.67 (s, 1 H, 7H, D_2O exchanged).

***N*-(4-Methoxyphenyl)-*N*,2-dimethyl-7*H*-pyrrolo[2,3-*d*]pyrimidin-4-amine (1).** To a solution of compound **11** (5 mmol, 0.84 g) in isopropanol (4 mL) was added 4-methoxy-*N*-methylaniline **12** (5.5 mmol, 0.75 g) and a drop of conc. HCl. The reaction mixture was refluxed for 4 h. After evaporation of the solvents, a silica gel plug (2 g) was made and loaded to a silica gel column. The column was eluted sequentially with 0% and 1% methanol in chloroform. Fractions containing the product (TLC) were pooled and evaporated to afford **1** as a white solid (1.14 g, 85%). R_f 0.60 (CH_3OH:$CHCl_3$ = 1:5); mp, 229.3−229.5 °C. ^{1}H NMR (DMSO-d_6): δ 2.45 (s, 3 H, 2-CH_3), 3.45 (s, 3 H, NCH_3), 3.82 (s, 3 H, OCH_3), 4.52 (d, 1 H, 5-H, J = 3.50 Hz), 6.73 (d, 1 H, 6-H, J = 3.55 Hz), 7.04 (d, 2 H, phenyl, J = 8.85 Hz), 7.27 (d, 2 H, phenyl, J = 8.85 Hz), 11.27 (s, 1 H, 7-H, D_2O exchanged). HRMS m/z calcd for $C_{15}H_{17}N_4O$ $[M + H]^+$, 269.1397; found, 269.1385 $[M + H]^+$. Anal. ($C_{15}H_{16}N_4O$) C, H, N.

***N*-(4-Methoxyphenyl)-*N*,2-dimethyl-7*H*-pyrrolo[2,3-*d*]pyrimidin-4-amine·HCl (1·HCl).** The HCl salt of **1** was obtained by treating its ether/ethyl acetate solution with HCl gas in an ice bath for 5 min. The white salt as it formed precipitated from the solution. The salt was collected and dried to give a white solid; mp 247.5−249.7 °C. ^{1}H NMR (DMSO-d_6): δ 2.64 (s, 3 H, 2-CH_3), 3.62 (s, 3 H, NCH_3), 3.81 (s, 3 H, OCH_3), 4.59 (s, 1 H, 5-H), 7.00 (s, 1 H, 6-H), 7.12 (d, 2 H, phenyl, J = 8.45 Hz), 7.41 (d, 2 H, phenyl, J = 8.30), 12.32 (s, 1 H, 7-H, D_2O exchanged). Anal. ($C_{15}H_{16}N_4O$) C, H, N.

***N*-(4-Methoxyphenyl)-2-methyl-7*H*-pyrrolo[2,3-*d*]pyrimidin-4-amine (2).** The synthesis of **2** followed the same method as for **1** using **11** (5 mmol, 0.84 g) and 4-methoxy-*N*-methylaniline **12** (5.5 mmol, 0.68 g). After column chromatography with 0% and 1% methanol in chloroform, fractions containing the product (TLC) were pooled and evaporated to afford **2** as a white solid (0.95 g, 75%). R_f 0.42 (CH_3OH:$CHCl_3$ = 1:5); mp, 258.7−259.9 °C. ^{1}H NMR (DMSO-d_6): δ 2.42 (s, 3 H, 2-CH_3), 3.73 (s, 3 H, OCH_3), 6.55 (d, 1 H, 5-H, J = 3.24 Hz), 6.91 (d, 2 H, phenyl, J = 8.96 Hz), 7.05 (d, 1 H, 6-H, J = 3.44 Hz), 7.74 (d, 2 H, phenyl, J = 8.92 Hz), 9.02 (s, 1H, N−H), 11.41 (s, 1 H, 7-H, D_2O exchanged). HRMS m/z calcd for $C_{14}H_{15}N_4O$ $[M + H]^+$, 255.1240; found, 255.1234 $[M + H]^+$. Anal. ($C_{14}H_{14}N_4O$) C, H, N.

2,6-Dimethyl-6,7-dihydro-3*H*-cyclopenta[*d*]pyrimidin-4(5*H*)-one ((±)-14). 3-Methyladipic acid (±)-**13** (1.60 g, 10 mmol) was heated at reflux in ethanol/conc. sulfuric acid solution (35 mL, v/v = 2.5/1) for 8 h. The solution was neutralized with ammonium hydroxide to pH = 7 and then diluted with ethyl acetate (100 mL) and washed with water. The organic phase was dried with anhydrous sodium sulfate and evaporated to afford a light yellow liquid which was used in the next step without further purification. The yellow liquid was dissolved in anhydrous toluene (100 mL), and sodium (0.23 g) was added to the solution. The mixture was heated at reflux for 3 h and cooled, neutralized with 1 N hydrochloric acid solution, and washed with water. After drying with anhydrous sodium sulfate, the organic phase was separated and evaporated to afford a light brown liquid. The liquid was used in the next step without further purification. The light brown liquid was diluted with *t*-BuOH. Acetamidine hydrochloride (1.13 g, 12 mmol) and potassium *tert*-butoxide (1.34 g, 12 mmol) were added, and the mixture was heated at reflux overnight. The reaction mixture was cooled, and the precipitate was collected by filtration. The residue was washed with warm methanol twice (30 mL × 1, 15 mL × 1). The filtrate and washings were combined, and then 3 g of silica gel was added and removed the solvent in vacuo to afford a dry plug. This plug was placed on the top of a silica gel column and eluted with 1% methanol in chloroform. Fractions containing the product were pooled and evaporated to afford 0.35 g of (±)-**14** (21% yield total for three steps) as a white solid. TLC R_f 0.30 ($CHCl_3$/CH_3OH, 10:1); mp 173.9−175.4 °C. ^{1}H NMR (DMSO-d_6): δ 1.05−1.07 (d, 3 H, CH_3, J = 6.8 Hz), 2.24 (s, 3 H, CH_3), 2.13−2.34, 2.73−2.90 (m, 5 H, CH_2CHCH_2), 12.16 (br, 1 H, OH, exchanged). Anal. ($C_9H_{12}N_2O$) C, H, N.

4-Chloro-2,6-dimethyl-6,7-dihydro-5*H*-cyclopenta[*d*]pyrimidine ((±)-15). A mixture of (±)-**14** (0.25 g, 1.5 mmol) and $POCl_3$ (10 mL) was heated at reflux for 3 h. The reaction mixture was cooled and evaporated at reduced pressure. The residue was diluted with

chloroform (50 mL) and neutralized with ammonium hydroxide slowly in an ice bath. The organic portion was washed with water (3 × 30 mL) and dried with anhydrous sodium sulfate. Concentration of the organic solvent with 1 g of silica gel afforded a dry plug. This plug was placed on the top of a silica gel column and eluted with 20% hexane in chloroform. Fractions containing the product were pooled and evaporated to afford 0.14 g of (±)-**15** as a colorless liquid (69%). Compound (±)-**15** was unstable and was used for the next step without further characterization.

General Procedure for (±)-3−(±)-7. Compound (±)-**15** and aniline or the appropriate substituted *N*-methyl anilines were dissolved in isopropanol (5 mL). To this solution was added 37% hydrochloric acid (2−3 drops). The mixture was heated at reflux for 3−6 h. Then the reaction was cooled and evaporated at reduced pressure. The residue was diluted with chloroform, neutralized with ammonium hydroxide, and then washed with water (2 × 30 mL). After drying with anhydrous sodium sulfate, organic solvent with 1 g of silica gel was evaporated under reduced pressure to give a dry plug. This plug was placed on the top of a silica gel column and eluted with chloroform. Fractions containing the product were pooled and evaporated to afford pure compounds (±)-**3**−(±)-**7**. Compounds were dissolved in anhydrous ether (10 mL), and then anhydrous hydrochloric acid gas was bubbled into the solution until no more solid precipitated out. The white solid was collected by filtration and dried over P_2O_5 to afford (±)-**3**·HCl, (±)-**5**·HCl−(±)-**7**·HCl.

***N*-(4-Methoxyphenyl)-*N*,2,6-trimethyl-6,7-dihydro-5*H*-cyclopenta[*d*]pyrimidin-4-aminium chloride ((±)-3·HCl).** Compound (±)-**3** was synthesized from (±)-**15** (0.19 g, 1.01 mmol) and 4-methoxy-*N*-methyl aniline (0.17 mg, 1.22 mmol) using the general procedure described above to afford after purification 0.18 g (61%) as a light yellow liquid. TLC R_f 0.24 ($CHCl_3$/CH_3OH, 10:1). Compound (±)-**3**·HCl was synthesized from (±)-**3** as a white solid (0.16 g, 79%); mp 196−198 °C. ^{1}H NMR (DMSO-d_6): δ 0.85−0.86 (d, 3 H, CH_3, J = 6.8 Hz), 1.37−1.47 (m, 1 H, CH), 1.89−1.99 (m, 1 H, CH), 2.26−2.35 (m, 1 H, CH), 2.43−2.44 (m, 1 H, CH), 2.98−3.05 (m, 1 H, CH), 2.60 (s, 3 H, 2-CH_3), 3.51 (s, 3 H, NCH_3), 3.80 (s, 3 H, OCH_3), 7.01−7.03 (d, 2 H, Ph-H, J = 8.8 Hz), 7.33−7.35 (d, 2 H, Ph-H, J = 8.8 Hz), 14.88 (br, 1 H, HCl, exch). Anal. ($C_{17}H_{22}N_3OCl$) C, H, N, Cl.

***N*-(4-Methoxyphenyl)-2,6-dimethyl-6,7-dihydro-5*H*-cyclopenta[*d*]pyrimidin-4-amine ((±)-4).** Compound (±)-**4** was synthesized from (±)-**15** (0.17 g, 0.94 mmol) and 4-methoxyaniline (0.14 g, 1.13 mmol) using the general procedure described above to afford after purification 0.16 g (61%) as a white solid. TLC R_f 0.32 ($CHCl_3$/CH_3OH, 10:1); mp 130.5−131.3 °C. ^{1}H NMR (DMSO-d_6): δ 1.09−1.12 (d, 3 H, CH_3, J = 6.8 Hz), 2.35 (s, 3 H, 2-CH_3), 1.36−1.48 (m, 1 H, CH), 1.88−2.01 (m, 1 H, CH), 2.25−2.35 (m, 1 H, CH), 2.41−2.45 (m, 1 H, CH), 2.98−3.05 (m, 1 H, CH), 3.73 (s, 3 H, OCH_3), 6.86−6.89 (d, 2 H, Ph-H, J = 8.8 Hz), 7.60−7.63 (d, 2 H, Ph-H, J = 8.8 Hz), 8.41 (br, 1 H, NH, exchanged). Anal. ($C_{16}H_{19}N_3O$) C, H, N.

***N*-(3-Methoxyphenyl)-*N*,2,6-trimethyl-6,7-dihydro-5*H*-cyclopenta[*d*]pyrimidin-4-aminium chloride ((±)-5·HCl).** Compound (±)-**5** was synthesized from (±)-**15** (0.23 g, 1.3 mmol) and 3-methoxy-*N*-methylaniline (0.20 g, 1.4 mmol) using the general procedure described above to afford after purification as a light yellow liquid. TLC R_f 0.33 ($CHCl_3$/CH_3OH, 10:1). Compound (±)-**5**·HCl was synthesized from (±)-**5** as an off white solid (0.27 g, 66% for two steps); mp 209.6−210.7 °C. ^{1}H NMR (DMSO-d_6): δ 0.85−0.87 (d, 3 H, CH_3, J = 6.8 Hz), 1.44−1.50 (m, 1 H, CH), 1.95−2.01 (m, 1 H, CH), 2.26−2.35 (m, 1 H, CH), 2.45−2.48 (m, 1 H, CH), 3.00−3.07 (m, 1 H, CH), 2.62 (s, 3 H, 2-CH_3), 3.55 (s, 3 H, NCH_3), 3.78 (s, 3 H, OCH_3), 6.69−7.42 (m, 4 H, Ph-H), 15.21 (br, 1 H, HCl, exchanged). Anal. ($C_{17}H_{22}N_3OCl$·$0.1H_2O$) C, H, N, Cl.

***N*-(2-Methoxyphenyl)-*N*,2,6-trimethyl-6,7-dihydro-5*H*-cyclopenta[*d*]pyrimidin-4-aminium chloride ((±)-6·HCl).** Compound (±)-**6** was synthesized from (±)-**15** (0.24 g, 1.31 mmol) and 2-methoxy-*N*-methylaniline (0.18 g, 1.31 mmol) using the general procedure described above to afford after purification as a colorless liquid. R_f 0.37 ($CHCl_3$/CH_3OH, 10:1). Compound (±)-**6**·HCl was synthesized from (±)-**6** as a white solid (0.23 g, 55% for two steps); mp 148−149 °C. ^{1}H NMR (DMSO-d_6): δ 0.83−0.85 (d, 3 H, CH_3, J = 6.8 Hz), 1.31−1.39 (m, 1 H, CH), 1.82−1.93 (m, 1 H, CH), 2.26−2.31 (m, 1 H, CH), 2.43−2.46 (m, 1 H, CH), 2.99−3.07 (m, 1 H, CH), 2.62 (s, 3 H, 2-CH_3), 3.45 (s, 3 H, NCH_3), 3.79 (s, 3 H, OCH_3), 7.03−7.51 (m, 4 H, Ph-H), 15.09 (br, 1 H, HCl, exchanged). Anal. ($C_{17}H_{22}N_3OCl$·$0.1H_2O$) C, H, N, Cl.

***N*-Phenyl-*N*,2,6-trimethyl-6,7-dihydro-5*H*-cyclopenta[*d*]pyrimidin-4-aminium chloride ((±)-7·HCl).** Compound (±)-**7** was synthesized from (±)-**15** (0.18 g, 0.99 mmol) and *N*-methylaniline (0.11 g, 0.99 mmol) using the general procedure described above to afford after purification 0.21 g (83%) as a white solid. R_f 0.36 ($CHCl_3$/CH_3OH, 10:1); mp 112.6−113.2 °C. ^{1}H NMR (DMSO-d_6): δ 0.81−0.83 (d, 3 H, CH_3), 1.40−1.44, 1.86−2.26, 2.74−2.80 (m, 5 H, CH_2CHCH_2), 2.41 (s, 3 H, 2-CH_3), 3.37 (s, 3 H, NCH_3), 7.18−7.41 (m, 4 H, Ph-H). Anal. ($C_{16}H_{19}N_3$) C, H, N. Compound (±)-**7**·HCl was synthesized from (±)-**7** (0.17 g, 0.65 mmol) as a white solid (0.15 g, 79%); mp 263.2−264.6 °C. ^{1}H NMR (DMSO-d_6): δ 0.83−0.85 (d, 3 H, CH_3, J = 6.8 Hz), 1.35−1.42 (m, 1 H, CH), 1.81−1.91 (m, 1 H, CH), 2.24−2.32 (m, 1 H, CH), 2.42−2.45 (m, 1 H, CH), 2.99−3.05 (m, 1 H, CH), 2.61 (s, 3 H, 2-CH_3), 3.55 (s, 3 H, NCH_3), 7.41−7.53 (m, 4 H, Ph-H), 15.09 (br, 1 H, HCl, exch). Anal. ($C_{16}H_{20}ClN_3$) C, H, N, Cl.

Molecular Modeling and Computational Studies. The X-ray crystal structure of tubulin at 3.58 Å resolution was obtained from the protein database (PDB ID 1SA0[40]). This crystal structure contains the $\alpha\beta$ dimers of tubulin complexed with *N*-deacetyl-*N*-(2-mercaptoacetyl) colchicine (DAMA colchicine), a close structural analogue of colchicine.

Docking Procedure. Docking studies were performed using the docking suite of Molecular Operating Environment software (MOE 2008.10).[43] The PDB file was downloaded (www.pdb.org) and imported into MOE. The A and B subunits of the protein, along with the crystallized ligand, were retained, while the C, D, and E subunits, GTP, GDP, and Mg ions were deleted. After addition of hydrogen atoms, the protein was then "prepared" using the LigX function in MOE. LigX is a graphical interface and collection of procedures for conducting interactive ligand modification and energy minimization in the active site of a flexible receptor. In LigX calculations, the receptor atoms far from the ligand are held fixed (constrained not to move) while receptor atoms near the ligand (in the active site) are allowed to move but are subject to tether restraints that discourage gross movement. The procedure was performed with the default settings.

Ligands were built using the molecule builder function in MOE and were energy minimized to its local minima using the MMF94X forcefield to a constant (0.05 kcal/mol).

Ligands were docked into the active site of the prepared protein using the docking suite as implemented in MOE. The docking was restricted to the active site pocket residues using the Alpha triangle placement method. Refinement of the docked poses was carried out using the Forcefield refinement scheme and scored using the Affinity dG scoring system. Around 30 poses were returned for each compound at the end of each docking run. The docked poses were manually examined in the binding pocket to ensure quality of docking and to confirm absence of steric clashes with the amino acid residues of the binding pocket.

To validate the utility of MOE 2008.10 for docking ligands into the active site, DAMA colchicine, the native ligand in the crystal structure (PDB: 1SA0), was built using the molecule builder, energy minimized, and docked into the active site using the above parameters. The best docked pose of DAMA colchicine displayed an rmsd of 0.9531 Å compared with the crystal structure pose of DAMA colchicine. MOE 2008.10 was thus validated for our docking studies. Docking studies of the lead

compounds and selected proposed molecules were performed using the same procedure.

Coordinates of the binding models of the 15 known tubulin inhibitors reported by Nguyen et al.[41] were retrieved from the Supporting Information. The coordinates as well as the docked pose of (*R*)-**3** were imported and visualized using MOE 2008.10. A systematic conformational search was carried out using Sybyl X 1.1[51] using 5° increments. Molecules were built using the molecule builder function in MOE 2008.10 and were imported into Sybyl X 1.1 and energy minimized using the Tripos force-field with a distance-dependent dielecetric and the Powell conjugate gradient with a convergence criterion of 0.01 kcal/mol.

Cellular Studies. Effects of Compounds on Cellular Microtubules. A-10 cells were used to evaluate the effects of the compounds on interphase and mitotic microtubules using indirect immunofluorescence techniques, and the EC_{50} values were calculated from a minimum of three experiments as described previously.[25]

Sulforhodamine B (SRB) Assay. The SRB assay[37,38] was used to evaluate the antiproliferative and cytotoxic effects of the compounds against cancer cells as previously described.[39] MDA-MB-435 cells were obtained from the Lombardi Cancer Institute (Washington D.C.). SK-OV-3 and HeLa cells were purchased from the American Type Culture Collection (Manassas, VA). The methods used to generate and characterize the SK-OV-3 MDR-1-6/6 and WTβIII cell lines have been described.[39] The IC_{50} represents the mean of at least three independent experiments using triplicate points in each experiment.

In Vitro Tubulin Polymerization. Inhibition of tubulin polymerization was measured using the tubulin polymerization assay kit (Cytoskeleton Inc.) according to manufacturer's directions. Briefly, 300 μg of purified bovine brain tubulin was incubated with tubulin assembly buffer (80 mM Na-Pipes, pH 6.9, 1 mM EGTA, 1 mM $MgCl_2$, 10 mM GTP, and 10% glycerol) and the indicated drug in a final volume of 100 μL. The polymerization of purified tubulin into microtubules was monitored by absorbance at 340 nm at 37 °C in a Spectromax Plus 96-well plate spectrophotometer (Molecular Devices).

Cell Cycle Analysis. MDA-MB-435 cells were treated for 24 h with vehicle, **1**, or (±)-**3**·**HCl** or 12.5 nM paclitaxel as a positive control. Following drug treatment, the cells were harvested and stained with Krishan's reagent and analyzed using a FacsCalibur flow cytometer. The data are plotted as propidium iodide intensity versus the number of events.

Quantitative Tubulin Studies. Bovine brain tubulin was purified as described previously.[57] The assembly reaction mixtures contained 1.0 mg/mL (10 μM) tubulin, 0.8 M monosodium glutamate (pH of 2 M stock solution adjusted to pH 6.6 with HCl), 4% (v/v) dimethyl sulfoxide as compound solvent, varying compound concentrations, and, after a 15 min preincubation at 30 °C, 0.4 mM GTP. The 0 °C reaction mixtures were transferred to 0 °C cuvettes in a recording spectrophotometer equipped with an electronic temperature controller. After baselines were established, the temperature was jumped to 30 °C over about 30 s, and changes in turbidity were measured over 20 min. The compound concentration that caused a 50% reduction in increase in turbidity, interpolated from the values obtained with defined compound concentrations, was defined as the IC_{50} value.[58] The assay to measure inhibition of [^{3}H]colchicine binding was described in detail previously.[59] Reaction mixtures contained 0.1 mg/mL (1.0 μM) tubulin, 5.0 μM [^{3}H]colchicine, and potential inhibitors at 1.0 or 5.0 μM, as indicated. Incubation was for 10 min at 37 °C, at which point the reaction has reached 40−60% of the maximum colchicine that can be bound in reaction mixtures without inhibitor. The [^{3}H]colchicine was a product of Perkin-Elmer. CA4 was a generous gift of Dr. G. R. Pettit, Arizona State University.

Acknowledgment. This work was supported, in part, by the National Institutes of Health and National Cancer Institute Grant CA098850 (AG). We thank Desiree LeBouf and Cara Westbrook for excellent technical assistance. A.L.R. was supported by a Cowles Fellowship, and support from the CTRC Cancer Center Support Grant, CCSG (CA054174) (S.L.M.) is acknowledged.

Supporting Information Available: Results from elemental analysis: high resolution mass spectra (HRMS) (EI); high resolution mass spectra (HRMS) (ESI); and representation of cell cycle distribution data (Figure 4). This material is available free of charge via the Internet at http://pubs.acs.org.

References

(1) Jordan, M. A.; Wilson, L. Microtubules as a Target for Anticancer Drugs. *Nat. Rev. Cancer* **2004**, *4*, 253–265.
(2) Jordan, M. A.; Kamath, K. How do Microtubule-Targeted Drugs Work? An Overview. *Curr. Cancer Drug Targets* **2007**, *7*, 730–742.
(3) Lee, J. F. Harris, L. N. Antimicrotubule Agents. In *Cancer: Principles & Practice of Oncology*, 8th ed.; DeVita, V. T., Jr., Lawrence, T. S., Rosenberg, S. A., Eds.; Lippincott Williams & Wilkins: Philadelphia, PA, 2008; pp 447−456.
(4) Löwe, J.; Li, H.; Downing, K. H.; Nogales, E. Refined Structure of $\alpha\beta$-Tubulin at 3.5Å Resolution. *J. Mol. Biol.* **2001**, *313*, 1045–1057.
(5) Huey, R. M.; Calvo, E.; Barasoain, I.; Pineda, O.; Edler, M. C.; Matesanz, R.; Cerezo, G.; Vanderwal, C. D.; Day, B. W.; Sorensen, E. J.; Lopez, J. A.; Andreu, J. M.; Hamel, E.; Diaz, J. F. Cyclostreptin Binds Covalently to Microtubule Pores and Lumenal Taxoid Binding Sites. *Nat. Chem. Biol.* **2007**, *3*, 117–125.
(6) Kanthou, C.; Tozer, M. T. Microtubule Depolymerizing Vascular Disrupting Agents: Novel Therapeutic Agents for Oncology and Other Pathologies. *Int. J. Exp. Pathol.* **2009**, *90*, 284–294.
(7) Carlson, R. O. New Tubulin Targeting Agents Currently in Clinical Development. *Expert Opin. Investig. Drugs* **2008**, *17*, 707–722.
(8) O'Connor, P. M.; Jackman, J.; Bae, I.; Myers, T. G.; Fan, S.; Mutoh, M.; Scudiero, D. A.; Monks, A.; Sausville, E. A.; Weinstein, J. N.; Friend, S.; Fornace, A. J., Jr.; Kohn, K. W. Characterization of the p53 Tumor Suppressor Pathway in Cell Lines of the National Cancer Institute Anticancer Drug Screen and Correlations with the Growth-inhibitory Potency of 123 Anticancer Agents. *Cancer Res.* **1997**, *57*, 4285–4300.
(9) Risinger, A. L.; Giles, F. J.; Mooberry, S. L. Microtubule Dynamics as a Target in Oncology. *Cancer Treat. Rev.* **2008**, *35*, 255–261.
(10) Hamel, E. An Overview of Compounds That Interact With tubulin and their Effects on Microtubule Assembly. In *The Role of Microtubules in Cell Biology, Neurobiology and Oncology*; Fojo, T., Ed.; Humana Press: Totowa, NJ, 2008; pp 1−19.
(11) Ling, V. Multidrug Resistance: Molecular Mechanisms and Clinical Relevance. *Cancer Chemother.* **1997**, *40*, S3–8.
(12) Leonard, G. D.; Fojo, T.; Bates, S. E. The Role of ABC Transporters in Clinical Practice. *Oncologist* **2003**, *8*, 411–424.
(13) Yeh, J. J.; Hsu, W. H.; Wang, J. J.; Ho, S. T.; Kao, A. Predicting Chemotherapy Response to Taxol-based Therapy in Advanced Non-Small-Cell Lung Cancer with P-glycoprotein Expression. *Respiration* **2003**, *70*, 32–35.
(14) Chiou, J. F.; Liang, J. A.; Hsu, W. H.; Wang, J. J.; Ho, S. T.; Kao, A. Comparing the Relationship of Taxol-based Chemotherpay Response with P-glycoprotein and Lung Resistance-related Protein Expression in Non-Small Cell Lung Cancer. *Lung* **2003**, *181*, 267–273.
(15) Nooter, K.; Westerman, A. M.; Flens, M. J.; Zaman, G. J.; Scheper, R. J.; van Wingerden, K. E.; Burger, H.; Oostrum, R.; Boersma, T.; Sonneveld, P. Expression of the Multidrug Resistance-Associated Protein (MRP) Gene in Human Cancers. *Clin. Cancer Res.* **1995**, *1*, 1301–1310.
(16) Fojo, T.; Menefee, M. Mechanisms of Multidrug Resistance: The Potential Role of Microtubule-stabilizing Agents. *Ann. Oncol.* **2007**, *18*, 3–8.
(17) Rosell, R.; Scagliotti, G.; Danenberg, K. D.; Lord, R. V. N.; Bepler, G.; Novello, S.; Cooc, J.; Crino, L.; Sanchez, J. J.; Taron, M.; Boni, C.; De Marinis, F.; Tonato, M.; Marangolo, M.; Gozzelino, F.; Di Costanzo, F.; Rinaldi, M.; Salonga, D.; Stephens, C. Transcripts in Pretreatment Biopsies From A Three-Arm Randomized Trial In Metastatic Non-Small-Cell Lung Cancer. *Oncogene* **2003**, *22*, 3548–3553.

(18) Dumontet, C.; Isaac, S.; Souquet, P.-J.; Bejui-Thivolet, F.; Pacheco, Y.; Peloux, N.; Frankfurter, A.; Luduena, R.; Perol, M. Expression of Class III Beta Tubulin In Non-Small Cell Lung Cancer Is Correlated With Resistance To Taxane Chemotherapy. *Bull. Cancer* **2005**, *92*, E25–30.
(19) Seve, P.; Isaac, S.; Tredan, O.; Souquet, P.-J.; Pacheco, Y.; Perol, M.; Lafanechere, L.; Penet, A.; Peiller, E.-L.; Dumontet, C. Expression of Class III β -Tubulin Is Predictive of Patient Outcome in Patients with Non-Small Cell Lung Cancer Receiving Vinorelbine-Based Chemotherapy. *Clin. Cancer Res.* **2005**, *11*, 5481–5486.
(20) Tommasi, S.; Mangia, A.; Lacalamita, R.; Bellizzi, A.; Fedele, V.; Chiriatti, A.; Thomssen, C.; Kendzierski, N.; Latorre, A.; Lorusso, V.; Schittulli, F.; Zito, F.; Kavallaris, M.; Paradiso, A. Cytoskeleton and Paclitaxel Sensitivity In Breast Cancer: The Role Of Beta-Tubulins. *Int. J. Cancer* **2007**, *120*, 2078–2085.
(21) Mozzetti, S.; Ferlini, C.; Concolino, P.; Filippetti, F.; Raspaglio, G.; Prislei, S.; Gallo, D.; Martinelli, E.; Ranelletti, F. O.; Ferrandina, G.; Scambia, G. Class III β-tubulin Overexpression Is A Prominent Mechanism Of Paclitaxel Resistance In Ovarian Cancer Patients. *Clin. Cancer Res.* **2005**, *11*, 298–305.
(22) Ferrandina, G.; Zannoni, G. F.; Martinelli, E.; Paglia, A.; Gallotta, V.; Mozzetti, S.; Scambia, G.; Ferlini, C. Class III β -Tubulin Overexpression Is A Marker Of Poor Clinical Outcome In Advanced Ovarian Cancer Patients. *Clin. Cancer Res.* **2006**, *12*, 2774–2779.
(23) Seve, P.; Dumontet, C. Is Class III β-Tubulin a Predictive Factor in Patients Receiving Tubulin-binding Agents? *Lancet Oncol.* **2008**, *9*, 168–175.
(24) Strengel, C; Newman, S. P.; Lesse, M. P.; Potter, B. V. L.; Reed, M. J.; Purohit, A. Class III Beta- Tubulin Expression and in vitro Resistance To Microtubule Targeting Agents. *Br. J. Cancer* **2010**, *102*, 316–324.
(25) Lee, L.; Robb, L. M.; Lee, M.; Davis, R.; Mackay, H.; Chavda, S.; O'Brien, E. L.; Risinger, A. L.; Mooberry, S. L.; Lee, M. Design, Synthesis and Biological Evaluations of 2,5-Diaryl-2,3-dihydro-1,3,4-oxadiazoline Analogs of Combretastatin-A4. *J. Med. Chem.* **2010**, *53*, 325–334.
(26) Dumontet, C.; Jordan, M. A.; Lee, F. F. Y. Ixabepilone: Targeting βIII-Tubulin Expression in Taxane-resistant Malignancies. *Mol. Cancer Ther.* **2009**, *8*, 17–25.
(27) Speicher, L. A.; Barone, L; Tew, K. D. Combined Antimicrotubule Activity of Estramustine and Taxol in Human Prostate Carcinoam Cell lines. *Cancer Res.* **1992**, *52*, 4433–4440.
(28) Giannakakou, P.; Villalba, L.; Li, H.; Poruchynsky, M.; Fojo, T. Combinations of Paclitaxel and Vinblastine and Their Effects on Tubulin Polymerization and Cellular Cytotoxicity: Characterization of a Synergistic Schedule. *Int. J. Cancer* **1998**, *75*, 57–63.
(29) Shi, W.; Horsman, M. R.; Siemann, D. W. Combined Modality Approaches Using Vasculature-disrupting Agents. In *Vascular-Targeted Therapies in Oncology*; Siemann, D. W., Ed.; J. Wiley & Sons, Ltd.: West Sussex, England, 2006; pp 123−136 and other chapters in the text.
(30) Gangjee, A.; Zhao, Y.; Ihnat, M. A.; Green, D. Miller, W. T. Synthesis of 2-Amino-4-*m*-bromoanilino-6-arylmethyl-7*H*-pyrrolo-[2,3-*d*]pyrimidines as Tyrosine Kinase Inhibitors and Antiangiogenic Agents. Presented at the 96th American Association for Cancer Research (AACR) Annual Meeting, Anaheim, CA, April 16−20, **2005**. Poster No. 3946.
(31) Gangjee, A.; Zhao, Y.; Raghavan, S.; Ihnat, M. A.; Disch, B. C. Design, Synthesis and Evaluation of 2-Amino-4-*m*-bromoanilino-6-arylmethyl-7*H*-pyrrolo[2,3-*d*]pyrimidines as Tyrosine Kinase Inhibitors and Antiangiogenic Agents. *Bioorg. Med . Chem.* **2010**, *18*, 5261–5273.
(32) Bai, R.; Paull, K. D.; Herald, C. L.; Pettit, G. R.; Hamel, E. Halichondrin B and Homohalichondrin B, Marine Natural Products Binding in the Vinca Domain of Tubulin. Discovery of Tubulin-based Mechanism of Action by Analysis of Differential Cytotoxicity Data. *J. Biol. Chem.* **1991**, *266*, 15882–15889.
(33) Paull, K. D.; Lin, C. M.; Malspeis, L.; Hamel, E. Identification of Novel Antimitotic Agents Acting at the Tubulin Level by Computer-assisted Evaluation of Differential Cytotoxicity Data. *Cancer Res.* **1992**, *52*, 3892–3900.
(34) Paull, K. D.; Hamel, E.; Malspeis, L. The Prediction of Biochemical Mechanism of Action From the in vivo Antitumor Screen of the National Cancer Institute. In *Cancer Chemotherapeutic Agents*; Foye, W. O., Ed.; American Chemical Society: Washington, DC, 1995; pp 9−45.
(35) West, R. A.; Beauchamp, L. 2-Alkyl(aryl)- and 2,7-Dimethyl-4-substituted Aminopyrrolo [2,3-*d*] pyrimidines. *J. Org. Chem.* **1961**, *26*, 3809–3812.
(36) Ohno, S.; Mizukoshi, K.; Komatsu, O.; Kuno, Y.; Nakamura, Y.; Kato, E.; Nagasaka, M. Synthesis and Hypoglycemic Activity of 7,8-Dihydro-6H-thiopyrano[3,2-*d*]pyrimidine Derivatives and Related Compounds. *Chem. Pharm. Bull.* **1986**, *34*, 4150–4165.
(37) Skehan, P.; Storeng, R.; Scudiero, D.; Monks, A.; McMahon, J.; Vistica, D.; Warren, J. T.; Bokesch, H.; Kenney, S.; Boyd, M. R. New Colorimetric Cytotoxicity Assay for Anticancer-Drug Screening. *J. Natl. Cancer Inst.* **1990**, *82*, 1107–1112.
(38) Boyd, M. R.; Paull, K. D. Some Practical Considerations and Applications of the National Cancer Institute *in vitro* Anticancer Discovery Screen. *Drug Dev. Res.* **1995**, *34*, 91–109.
(39) Risinger, A. L.; Jackson, E. M.; Polin, L. A.; Helms, G. L.; LeBoeuf, D. A.; Joe, P. A.; Hopper-Borge, E; Ludueña, R. F.; Kruh, G. D.; Mooberry, S. L. The Taccalonolides: Microtubule Stabilizers that Circumvent Clinically Relevant Taxane Resistance Mechanisms. *Cancer Res.* **2008**, *68*, 8881–8888.
(40) Ravelli, R. B. G.; Gigant, B.; Curmi, P. A.; Jourdain, I.; Lachkar, S.; Sobel, A.; Knossow, M. Insight into Tubulin Regulation from a Complex with Colchicine and a Stathmin-like Domain. *Nature* **2004**, *428*, 198–202.
(41) Nguyen, T. L.; McGrath, C.; Hermone, A. R.; Burnett, J. C.; Zaharevitz, D. W.; Day, B. W.; Wipf, P.; Hamel, E.; Gussio, R. A Common Pharmacophore for a Diverse Set of Colchicine Site Inhibitors Using a Structure-based Approach. *J. Med. Chem.* **2005**, *48*, 6107–6116.
(42) Bhattacharyya, B.; Panda, D.; Gupta, S.; Banerjee, M. Anti-Mitotic Activity of Colchicine and the Structural Basis for its Interaction with Tubulin. *Med. Res. Rev.* **2008**, *28*, 155–183.
(43) *Molecular Operating Environment* (*MOE 2008.10*); Chemical Computing Group, Inc.: Montreal, Quebec, Canada, 2008; www.chemcomp.com.
(44) De Martino, G.; La Regina, G.; Coluccia, A.; Edler, M. C.; Barbera, M. C. Arylthioindoles, Potent Inhibitors of Tubulin Polymerization. *J. Med. Chem.* **2004**, *47*, 6120–6123.
(45) Gangjee, A.; Devraj, R.; McGuire, J. J.; Kisliuk, R. L. 5-Arylthio Substituted 2-Amino-4-oxo-6-methylpyrrolo[2,3-*d*]pyrimidine Antifolates as Thymidylate Synthase Inhibitors and Antitumor Agents. *J. Med. Chem.* **1995**, *38*, 4495–4502.
(46) Gangjee, A.; Vasudevan, A.; Kisliuk, R. L. Nonclassical 5-Substituted Tetrahydroquinazolines as Potential Inhibitors of Thymidylate Synthase. *J. Heterocycl. Chem.* **1997**, *34*, 1669–1676.
(47) Gangjee, A.; Mavandadi, F.; Kisliuk, R. L.; Queener, S. F. Synthesis of Classical and a Nonclassical 2-Amino-4-oxo-6-methyl-5-substituted Pyrrolo[2,3-*d*]pyrimidine Antifolate Inhibitors of Thymidylate Synthase. *J. Med. Chem.* **1999**, *42*, 2272–2279.
(48) Gangjee, A.; Jain, H. D.; McGuire, J. J.; Kisliuk, R. L. Benzoyl Ring Halogenated Classical 2-Amino-6-methyl-3,4-dihydro-4-oxo-5-substituted Thiobenzoyl-7*H*-pyrrolo[2,3-*d*]pyrimidine Antifolates as Inhibitors of Thymidylate Synthase and as Antitumor Agents. *J. Med. Chem.* **2004**, *47*, 6730–6739.
(49) Gangjee, A.; Li, W.; Yang, J.; Kisliuk, R. L. Design, Synthesis, and Biological Evaluation of Classical and Nonclassical 2-Amino-4-oxo-5-substituted-6-methylpyrrolo[3,2-*d*]pyrimidines as Dual Thymidylate Synthase and Dihydrofolate Reductase Inhibitors. *J. Med. Chem.* **2008**, *51*, 68–76.
(50) Webber, S. J.; Bleckman, T. M.; Attard, J.; Deal, J. G.; Kathardekar, V.; Welsh, K. M.; Webber, S.; Janson, C. A.; Matthews, D. A. Design of Thymidylate Synthase Inhibitors Using Protein Crystal Structures: The Synthesis and Biological Evaluation of a Novel Class of 5-Substituted Quinazolinones. *J. Med. Chem.* **1993**, *36*, 733–746.
(51) *Sybyl X 1.1*; Tripos, Inc.: St. Louis, MO, 2010.
(52) Kasibhatla, S.; Baichwal, V.; Cai, S. X.; Roth, B.; Skvortsova, I.; Skvortsov, S.; Lukas, P.; English, N. M.; Sirisoma, N.; Drewe, J.; Pervin, A.; Tseng, B.; Carlson, R. O.; Pleiman, C. M. MPC-6827: A Small Molecule Inhibitor of Microtubule Formation that is not a Substrate for Multidrug Resistance Pumps. *Cancer Res.* **2007**, *67*, 5865–5871.
(53) Sirisoma, N.; Kasibhatla, S.; Pervin, A.; Zhang, H.; Jiang, S.; Willardsen, J. A.; Anderson, M.; Baichwal, V.; Mather, G. G.; Jessing, K.; Hussain, R.; Hoang, K.; Pleiman, C. M.; Tseng, B.; Drewe, J.; Cai, S. X. Discovery of 2-Chloro-*N*-(4-methoxyphenyl)-*N*-methylquinazolin-4-amine (EP128265, MPI-0441138) as a Potent Inducer of Apoptosis with High In Vivo Activity. *J. Med. Chem.* **2008**, *51*, 4771–4779.
(54) Sirisoma, N.; Pervin, A.; Zhang, H.; Jiang, S.; Willardsen, J. A.; Anderson, M.; Mather, G. G.; Pleiman, C. M.; Kasibhatla, S.; Tseng, B.; Drewe, J.; Cai, S. X. Discovery of *N*-(4-Methoxyphenyl)-*N*,2-dimethylquinazolin-4-amine, a Potent Apoptosis Inducer and Efficacious Anticancer Agent with High Blood Brain Barrier Penetration. *J. Med. Chem.* **2009**, *52*, 2341–2351.
(55) Sirisoma, N.; Pervin, A.; Zhang, H.; Jiang, S.; Willardsen, J. A.; Anderson, M.; Mather, G. G.; Pleiman, C. M.; Kasibhatla, S.; Tseng, B.; Drewe, J.; Cai, S. X. Discovery of *N*-methyl-4-(4-methoxyanilino) quinazolines as Potent Apoptosis Inducers.

Structure−Activity Relationship of the Quinazoline Ring. *Bioorg. Med. Chem. Lett.* **2010**, *20*, 2030–2334.
(56) Kemnitzer, W.; Sirisoma, N.; May, C.; Tseng, B.; Drewe, J.; Cai, S. X. Discovery of 4-Anilino-N-methylthieno[3,2-*d*]pyrimidines and 4-Anilino-N-methylthieno[2,3-d]pyrimidines as Potent Apoptosis Inducers. *Bioorg. Med. Chem. Lett.* **2009**, *19*, 3536–3540.
(57) Hamel, E.; Lin, C. M. Separation of Active Tubulin and Microtubule-associated Proteins by Ultracentrifugation and Isolation of a Component Causing the Formation of Microtubule bundles. *Biochemistry* **1984**, *23*, 4173–4184.
(58) Hamel, E. Evaluation of Antimitotic Agents by Quantitative Comparisons of Their Effects on the Polymerization of Purified Tubulin. *Cell Biochem. Biophys.* **2003**, *38*, 1–22.
(59) Verdier-Pinard, P.; Lai, J.-Y.; Yoo, H.-D.; Yu, J.; Márquez, B.; Nagle, D. G.; Nambu, M.; White, J. D.; Falck, J. R.; Gerwick, W. H.; Day, B. W.; Hamel, E. Structure-Activity Analysis of the Interaction of Curacin a, the Potent Colchicine Site Antimitotic Agent, with Tubulin and Effects of Analogs on the Growth of MCF-7 Breast Cancer Cells. *Mol. Pharmacol.* **1998**, *53*, 62–76.